

Spectroscopy of ε Aurigae during the 2009-2011 eclipse.

I. S. Potravnov^{1,2*}, V. P. Grinin^{1,2}

1 - Pulkovo Astronomical Observatory, Russian Academy of Sciences, 196140, Pulkovo, St. Petersburg, Russia

2 - The Sobolev Astronomical Institute, St. Petersburg University, Petrodvorets, St. Petersburg, Russia

Abstract

The results of the spectral observations of a unique eclipsing system ε Aurigae obtained during the recent eclipse are presented. We traced the spectral lines variations at different eclipse phases. The part of these changes is the result of the absorption of stellar radiation by the gas component of circumstellar (CS) disk around the secondary. The other part arises due to the obscuration of the stellar photosphere and the closest circumstellar area by the dusty CS disk. Comparison of our results with the previous one, obtained by Lambert & Sawyer during the 1982-1984 eclipse, indicates the good agreement, and argues in favor of stability of the secondary disk structure. On the base of the new observational data we provide a new mass estimation of the system components.

arXiv:1309.0370v1 [astro-ph.SR] 2 Sep 2013

* e-mail: <ilya.astro@gmail.com>

1 Introduction

ε Aur is one of the most enigmatic eclipsing binary system. Variability of this star was discovered by the pastor Fritch in 1821. However, only in 1903 Ludendorf showed that it is the eclipsing binary with the unusually long period: ~ 27.1 years. The duration of the eclipses is even more surprising: approximately two years. Together with the long orbital period it indicates that the size of the obscuring body is much larger than the largest known stellar diameters. Also it means the precise edge-on orientation of the orbital plane to the line of sight. The main component of the system is the bright F0 Ia supergiant ($V \sim 3.0^m$). Every 27 years it is occulted by the secondary component which does not manifest itself in the optical wavelengths range. Currently, due to the substantial distance uncertainty only the mass function of the system $f \sim 2.5M_\odot$ [1,2] is known. Therefore the term 'main' traditionally applies to the visible F star.

Two different types of the models of ε Aur were considered (e.g. [3] and the papers cited there). In one of them, so-called, 'massive' model, the optical component is the normal supergiant with the mass $M \sim 15M_\odot$, which has left recently the Main Sequence. In this case the secondary has the mass $M \sim 13M_\odot$. In the second, so-called, 'low-mass' model, the main component is an evolved post-AGB star with the mass close to $1 M_\odot$; the secondary is more massive: $M \sim 5M_\odot$. The common assumption for both these models is that the obscuring body is the CS disk of the secondary [4], that was confirmed by the interferometric observations during the last 2009-2011 eclipse [5].

The photospheric spectrum of the main component remains visible during the all eclipse phases. The additional spectral lines arise in the disk around the secondary and blend the spectrum of the primary. These lines have been observed beginning from the early spectroscopic investigations of the star. These lines appear in the ingress phase and disappear after the end of the eclipse [6]. The spectra of ε Aur obtained by Struve et al. [7] during the 1954-1957 eclipse confirmed this and demonstrated the complex variability of the spectral lines. Lambert & Sawyer [8] estimated the masses of the system components: $M_1 \leq 3M_\odot$ и $3 \leq M_2/M_\odot \leq 6$, using the K I 7699 Å radial velocity and the assumption that the secondary disk is the Keplerian one. It was the argument in favor of the 'low-mass' scenario.

During the 1982-1984 eclipse there were several attempts to distinguish the spectral lines which are formed in the disk of the secondary [9, 10]. It was shown that such lines had the excitation temperature $T \sim 4000K$ [10]. Thereby, in the spectrum of the primary the lines with the high excitation potential such as NI triplet, or the high members of the Paschen series do not exhibit the eclipse effects, and their radial velocities trace the orbital motion of the optical component.

Any attempts to observe the spectral lines of the secondary component were unsuccessful [11].

2 Observations and data reduction

The last eclipse of ε Aur occurred in 2009-2011. The result of the long term observations of the radial velocity were the updated orbital parameters and ephemeris [1, 2, 12]. Unfortunately, the argument of the pericenter is determined with some uncertainty because it is impossible to detect the secondary eclipse. The additional source of the uncertainty in the stellar parameters estimate are pulsations of the primary (see below). According to the results of the international observational campaign [13], the mid-eclipse in the V band occurred on 22.07.2010 (JD 2455400). The photometric moments of the eclipse phases are presented in Table 1.

Contact	Date	JD
I	16.08.2009	2455070
II	22.02.2010	2455250
III	27.02.2011	2455620
IV	26.08.2011	2455800

Table 1: The moments of the photometric contacts [13]

The spectra discussed in our paper were obtained using the high resolution ($R = 45000$) echelle spectrograph MAESTRO with the 2 m telescope at the Terskol Observatory. We obtained 58 spectra in the 3900-9800 Å wavelength range during the time range from 03.04.2009 to 30.11.2012. Our observations cover practically all eclipse phases except the moment of egress, when observations could not be fulfilled due to the technical problems. The comparison between the out of eclipse spectra and the spectra obtained during

the eclipse provide an opportunity to trace the spectral changes arising due to the passage of the secondary's circumstellar disc across the line of sight. The standard procedure of the spectroscopic data reduction was fulfilled with the IRAF software package [14]. The wavelength calibration has been done using the Th-Ar lamp comparison spectra obtained during each observation night. The heliocentric correction was applied. The continuum normalization of spectral orders has been done using the spline approximation of the manually determined points. This allows us to take accurately into account the broad wings of some spectral lines. The further analysis of the spectra, including the measurement of the radial velocities and lines equivalent widths, has been done using the DECH 30 software [15].

3 Results

3.1 KI 7699 Å line

The resonance potassium doublet KI 7664 Å and 7699 Å absent in the photospheric spectrum of the main component. The weak lines of this doublet which we observed in the out of eclipse spectra had the interstellar origin [16]. Nevertheless, these lines demonstrate the strong variability during the eclipse. This variability arises due to scattering of the photospheric radiation by the neutral potassium atoms in the disk of the secondary. Therefore, the investigation of this variability reveals the dynamics of the gas component in the disk. A comprehensive analysis of the KI 7699 Å variability during the 1982-1984 eclipse presented by Lambert & Sawyer [8]. Unlike to the stronger KI 7664 Å line, this line is less affected by the telluric O₂ spectrum. Therefore, for our analysis we chose the KI 7699 Å line. Figure 1 demonstrates the consequence of changes in this line during the eclipse. For simplicity, we show only part of the spectral line profiles for selected eclipse phases.

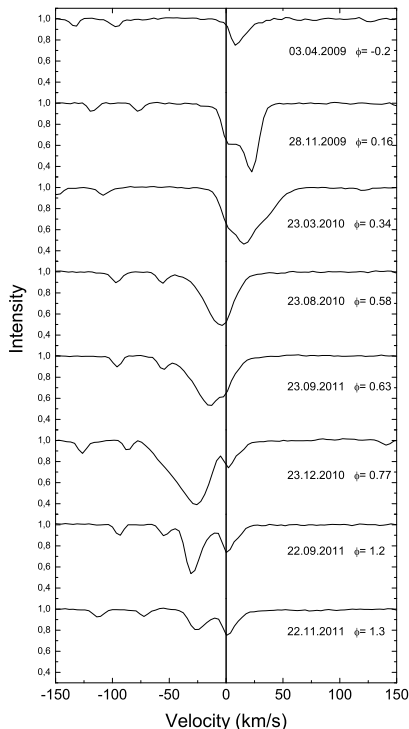


Figure 1: The KI 7699 Å line profiles variability during the eclipse. Two weak absorption lines at the blue part of plots are the telluric lines. Their shift is the result of the heliocentric correction.

The X-axis is the phase of the eclipse ϕ . The zero point is the moment of the first photometric contact (duration of the eclipse is accepted as a unit). On the first out of eclipse spectrum, the weak interstellar potassium line is clearly seen. However, just after the beginning of the eclipse the additional strong redshifted absorption has appeared. On the following spectra this absorption became stronger and gradually

merged with the interstellar component. Close to the mid-eclipse phase the profile of this blend demonstrates a small asymmetry of the blue wing, which evolves into the separate absorption component. In the last two profiles obtained at the end of the eclipse this additional absorption became weaker.

Variability of the KI 7699 Å line equivalent width (EW(KI)) is shown in Fig. 2. The dependence of EW(KI) on the phase of eclipse reaches the maximum near the second and third contacts. There is a difference between an amplitude of these maxima: it is smaller near the second contact. Such an asymmetry appears also on the radial velocity curve (see below). The variability of EW(KI) arises because of the variations of the potassium atom column density in the CS disk of the secondary in the projection on the primary's disk. The comparison of our data with the data obtained by Lambert & Sawyer [8] during the previous eclipse shows the good agreement. According to their assumption, the difference in the EW(KI) amplitudes at the ingress and egress phases is due to the non-symmetric position of the central body in the circumstellar disk.

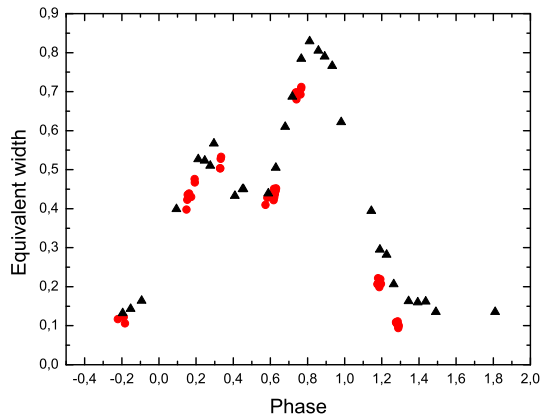


Figure 2: Variability of the KI 7699 Å line equivalent width during the eclipse (red circles). The data by Lambert & Sawyer [8] are marked by triangles.

Figure 3 demonstrates the KI radial velocity curve (RV(KI)) during the eclipse. We also see here the good agreement between the present and the previous RV curves. This argues in favor of the stability of the secondary circumstellar disk. When intersecting the line of sight, the rotating disk absorbs the radiation of the primary firstly at the red side of the interstellar line, and then at the blue side. At the second part of the eclipse an interesting detail is clearly seen (Fig. 1): an additional blue shifted absorption component appeared. It is save till the last phase of observations (November 2012) and possibly later. This indicates an existence of the gaseous matter on the line of sight after the end of the photometric eclipse. This matter may be the extended gaseous structure like a stream trailing behind the disk of the secondary. Such structures can appear in the evolved binary systems (see e.g. [17]).

3.2 The D Na I resonance lines

The sodium doublet 5889 Å and 5895 Å in ϵ Aurigae spectrum demonstrate a complex structure: the profiles consist of both interstellar and weak stellar components which originate in the photosphere of the primary. The contribution of the first component is more significant. Therefore, the sodium lines do not demonstrate any noticeable variability due to the primary pulsations. The spectral variability in the Na I lines during the eclipse (Fig. 4) was similar to that observed in the KI 7699 Å line. Due to the low excitation potentials, additional absorption components observed during the eclipse were formed at the similar physical conditions. In particular, as in the case of the KI 7699 Å line, the additional blue-shifted absorption component of the D NaI lines appeared after the middle of the eclipse and was observed after the end of the eclipse.

3.3 The FeII 4515 Å line

The lines of the ionized iron are widely presented in the spectrum of ϵ Aur. For an analysis we chose one of them, namely, the unblended FeII 4515 Å line. In general, the variability of this line is in a good agreement

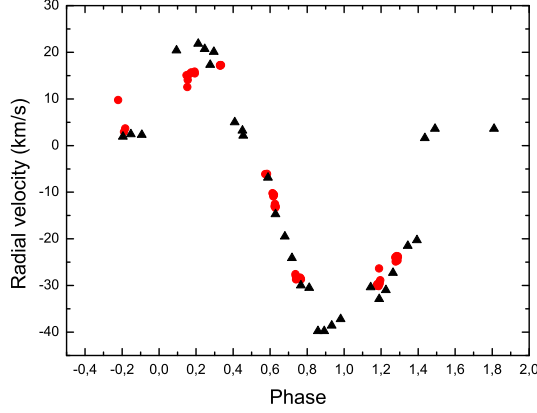


Figure 3: Behavior of the KI 7699 Å radial velocities during the eclipse (red circles). The data by Lambert & Sawyer [8] are marked by triangles.

with the previously described changes in the alkali metals line but in a smaller scale. The appearance of the red- and blue-shifted additional absorption is clearly traced in the ingress and egress phases correspondingly. Figure 5 presents the consequent changes in the line profile during the eclipse. In Fig. 6 we compare the radial velocity curves both in the FeII 4515 Å and KI 7699 Å lines. One can see a good general agreement in the behavior of these curves. However, some lag is clearly seen. At the phase $\phi \sim 0.2$ the KI radial velocity begins to grow due to the appearance of the additional red-shifted absorption. At the same time, the FeII radial velocity is still close to the orbital motion of the F star. The additional absorption in this line appears at the later phases of the eclipse, and disappears earlier. Near the end of the eclipse, the RV amplitude in the FeII 4515 Å line is lower than in the KI 7699 Å. After the end of the eclipse the radial velocity in the iron line quickly returns to the orbital one. This means that the formation region of this line is more compact in comparison with the KI line formation area.

3.4 The CaII K line

The CaII K resonance line proved to be quiet stable line in the ε Aur spectrum. The line profile looks practically the same at all phases of the eclipse (Fig. 7), and do not demonstrate any noticeable additional absorption associated with the disk of the secondary. This means that there is no enough amount of the calcium atoms in the disk around the secondary, which could cause the changes in the line profile during the eclipse. This fact is really surprising because this line is the resonance one, and calcium is one of the most abundant metal.

3.5 The NI and P 12 lines

Due to the high excitation potentials, we allocated the near-infrared nitrogen triplet NI 8703, 8711, 8718 Å and hydrogen Paschen 12 line in the separate group. These lines are formed in the photosphere of primary and do not demonstrate any effects caused by the eclipse. Thus, as mentioned above, the radial velocities measured in these lines, traced the orbital motion of the F star. Nevertheless, the nitrogen lines demonstrate a small variability. The gradual intensification observed in blue and red wings of the NI lines was not correlated with the eclipse phases. The similar changes in these lines has been observed by Lambert & Sawyer [8] during the previous eclipse. Such a variability is probably caused by the pulsations of ε Aur. It should be noted that this effect directly influences the precision of the radial velocity measurements. For the direct measurements of RV we choose the nitrogen line 8711 Å. Figure 8 shows the behavior of the radial velocity measured for this line at the different phases of the eclipse. We have obtained the same result using the Paschen 12 line. Due to the high excitation potential of the upper levels NI 8711 Å and Paschen 12 lines there are no additional absorption components arising in the disk of the secondary. This is the reason why the behavior of NI and Paschen lines radial velocities is noticeably different from RV(KI) (see Fig. 3).

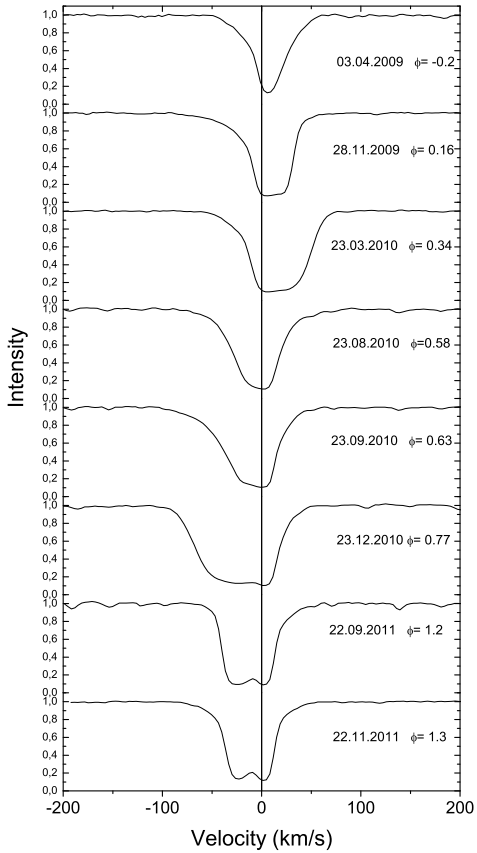


Figure 4: Changes in the NaI 5895 Å line profiles during the eclipse.

3.6 The Balmer lines H_α and H_δ

Out of eclipse, the H_α line demonstrates the absorption profile with two weak emission peaks at the both sides. Guangwei et al. [18] attributed formation of these peaks to the rotating ring-like structure around the primary which can be a result of the stellar wind. On the base of the radial velocities changes in the H_α line and the orbital velocity of the F star Chadima et al. [11] argued that the H_α emission is formed in the nearest vicinity of the primary.

Our observations show that the H_α line demonstrates significant changes during the eclipse (Fig. 9). On the earliest phases of the eclipse the additional red absorption appeared while the red emission peak gradually disappeared. At the mid-eclipse phase the profile is almost symmetric and strongly broad without any signs of the emission. On the egress phase the picture is unfolded in the reverse order. The additional absorption shifted to the blue side, and the blue emission peak disappeared while the red emission reappeared. At the end of the eclipse the profile returned to the shape observed out of eclipse.

The H_β line is strongly blended by the CrII line, so we excluded it from our analysis of the spectral variability. The H_δ line changes during the eclipse were in general similar to the H_α one. We see, however, no emission components in the H_δ line, and the line broadening at the middle of the eclipse was not so strong as in the H_α line (Fig. 10).

4 Discussion

As mentioned in the Introduction, the crucial question for understanding of ε Aur evolutionary status is the problem of the distance to the system. The distance directly measured by Hipparcos had the error comparable with the measured value of D . The revision of the Hipparcos catalogue fulfilled by van Leeuwen [19] gives the parallax value $\pi = 1.53 \pm 1.29$ that corresponds to the ε Aur distance $D = 653 \pm 551$ pc. Recently other two attempts to determine the distance to ε Aur have been undertaken. The first of them

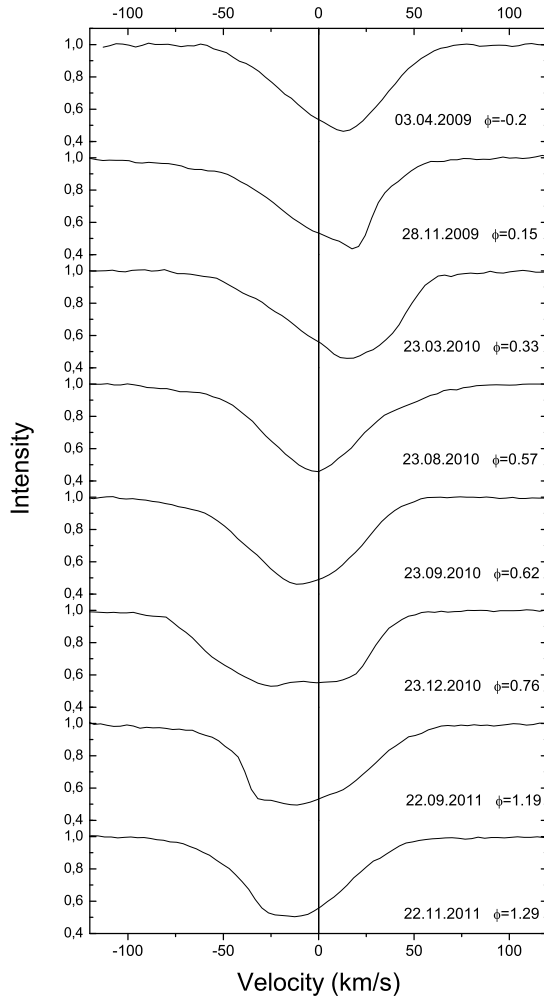


Figure 5: FeII 4515 Å line profiles variability during the eclipse.

[20] was based on the original method included the distance calibration as a function of the reddening and 6613 Å DIB intensity. This method was applied to the nearest to the ϵ Aur stars under the assumption about the sufficient homogeneity of the interstellar medium in the volume investigated. The authors of the paper [20] give the value $D = 1.5 \pm 0.5$ kpc. However, they have noted, that not very accurate photometric calibration due to the star pulsations and the influence of the circumstellar matter in the nearest vicinity of the system could exist. It should be also noted that taking into account this distance and the recent interferometric measurements of the diameter of the primary [1], we obtain the stellar radius in the range of $\sim 200 - 500 R_{\odot}$. Such radii are typical for the coldest Mira-like variables rather than for the F supergiants which radii are usually $R \sim 80 - 100 R_{\odot}$ [21]. The alternative estimate of D was fulfilled in the PhD thesis by Kloppenborg [1]. This estimate was based on the astrometric analysis of the plates from Sproul observatory collection during the 45-year period. Together with the new orbital parameters of the system, these data give the distance value $D = 737 \pm 67$ pc. This value is in a satisfactory agreement with the previous measurement by van de Kamp [22]. Nevertheless, this estimate was affected by the uncertainties in the astrometric parameters of the reference stars and insufficient precision of the orbital parameters. In the case when only one component of the binary system is observed it is really a difficult task.

A similarity in the behavior of the radial velocity and the equivalent width during the current and previous eclipses argue in favor of the general stability of the disk around the invisible companion. Using the KI 7699 Å radial velocity measurements and the velocity of the disk motion ($V_d \approx 30$ km/s) relatively to the F star recently obtained from the interferometric measurements [1,5] one can reconsider the mass of the secondary M_2 . For this purpose, we adopt the distance $D = 737$ pc [1] as the more probable value. Combining the

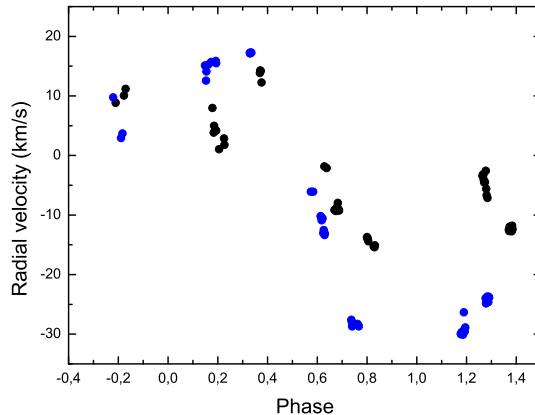


Figure 6: The radial velocities of the FeII 4515 Å (black circles) and KI 7699 Å (blue circles) lines during the eclipse.

velocity 30 km/s with the duration of the photometric eclipse from Table 1 we obtain the estimate of the disk diameter $D_{disk} \sim 12.5$ AU. The semi-amplitude of the KI 7699 Å radial velocity curve based on averaging our and Lambert & Sawyer [8] data is $K = 29.7$ km/s. Adopting this value as the Keplerian velocity at the distance from the unseen component $0.5D_{disk}$, we obtain $M_2 = 6.2M_{\odot}$. Substituting this value in the mass function equation, we obtain the mass of the primary: $M_1 = 3.5M_{\odot}$. Thus, the observations during the 2009-2011 eclipse confirmed the mass estimate by Lambert & Sawyer [8] and argue in favor of the 'low-mass' scenario.

It should be noted that observed rotation velocity is probably not the strictly Keplerian one. Besides, when we measure the line shift due to the disk rotation we observe the matter motion effect along the line of sight. This means that the resulting value of the velocity will be slightly less than the 'true' Keplerian velocity (at the disk radius). Correspondingly, the true mass can be slightly larger.

The low-mass scenario is also supported by Hoard et al. (2010). These authors' have shown that observed spectral energy distribution of ε Aur can be reproduced by the model with masses $2.2M_{\odot}$ and $5.9M_{\odot}$ for the primary and secondary components correspondingly. The ε Aur double-mode pulsation period $\approx 67^d$ and 123^d [24] is shorter, than in the case of the well-studied normal supergiant ρ Cas (≈ 1 year)[8]. At the same time the analysis of the chemical composition of ε Aur [25] demonstrates its similarity to the massive supergiants composition, but not to the post-AGB stars. It still seems difficult to make the final choice between two models without the more precise distance to the system.

For complete understanding of the ε Aur system it is very important to explain the possibility of the origin of the H_{α} line profile broadening up to 200 km/s near to the mid-eclipse. As was proposed in one of the earliest models, the disk around the secondary had the central hole [26]. It was necessary for the explanation of the little brightening in the light curve near the middle of the eclipse. However, in the disk model by Kloppenborg et al. [1,5], this hole is absent. Possibly, the sensitivity of their method was not enough to resolve this structure in the disk. However, it is quiet possible that this central hole is absent or can not be observed due to the edge-on orientation of the disk.

In this case, a projection of the dusty disk on the sky plane differs from the ellipse. According to the Lissauer et al. model [27], it could be something like the flared disk. In this model, the area of the H_{α} line broadening (Section 3.6.) locates close to the central region of the disk. It could be structure like the rapidly rotating hot halo above the disk plane or the magneto-centrifugal disk wind (if the disk has the magnetic field). In the Section 3.3 we also mentioned the lag between the changes in the FeII and the KI line profiles. This observational fact means the presence of the radial temperature gradient in the halo, mentioned above. In the next paper we are going to consider this effect in more detail.

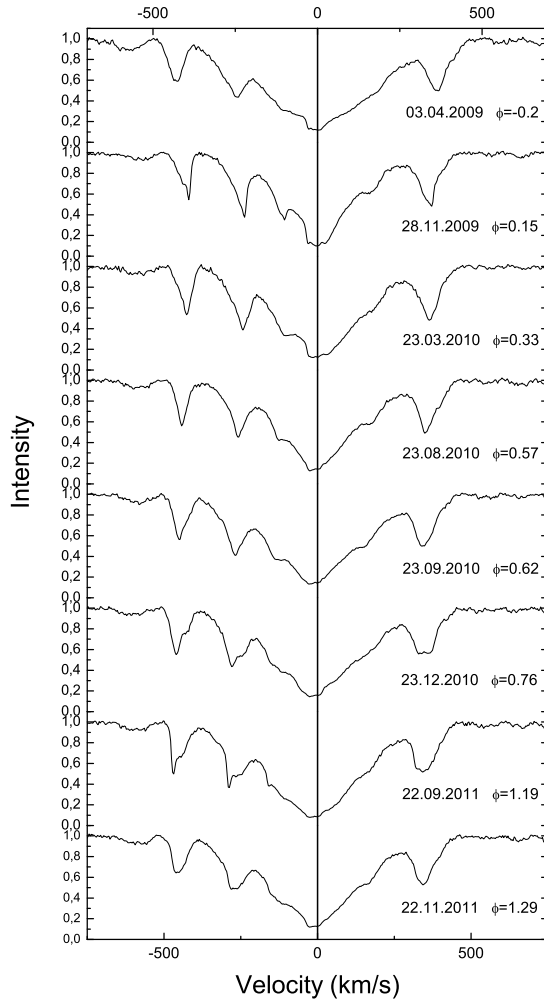


Figure 7: CaII K line profiles at the different eclipse phases.

5 Conclusion

The results of the spectroscopic observations during the last eclipse of ε Aur demonstrate a stability of the gaseous component of the disk around the secondary from eclipse to eclipse. The KI 7699 Å radial velocity curve is in a good agreement with the previous observations by Lambert & Sawyer [8], and argue in favor of the 'low-mass' model of ε Aur. The $H\alpha$ line profile broadening is the evidence of the presence of the hot rapidly rotating gas above the cold dusty disk. Its temperature increases toward the center. Projection of this area covers a significant part of the F star disk. The excitation state of the atomic levels is such that the gas can absorb the radiation of the primary at the $H\alpha$ line frequencies but it does not contribute to the emission in this line. This means that the excitation temperature in the $H\alpha$ line is lower than the ε Aur effective temperature (approximately 8000 K). Theoretical modelling of this region can reveal the source of its heating.

We thank the Terskol Observatory staff for the observations. This work was supported in part by the Basic Research Program P21 of the Presidium of the Russian Academy of Sciences, grant N.Sh. 1625.2012.2, and grant № 1.2.1 of Federal Targeted program 'Science and Science Education for Innovation in Russia 2012-2013'.

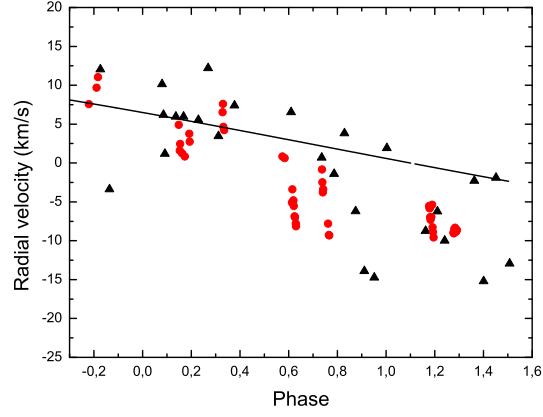


Figure 8: The variability in the NI 8711Å line radial velocity (red circles). The data by Lambert & Sawyer [8] are shown by triangles. The orbital motion of the primary was calculated on the base of the orbital solution [2] and shown by the line.

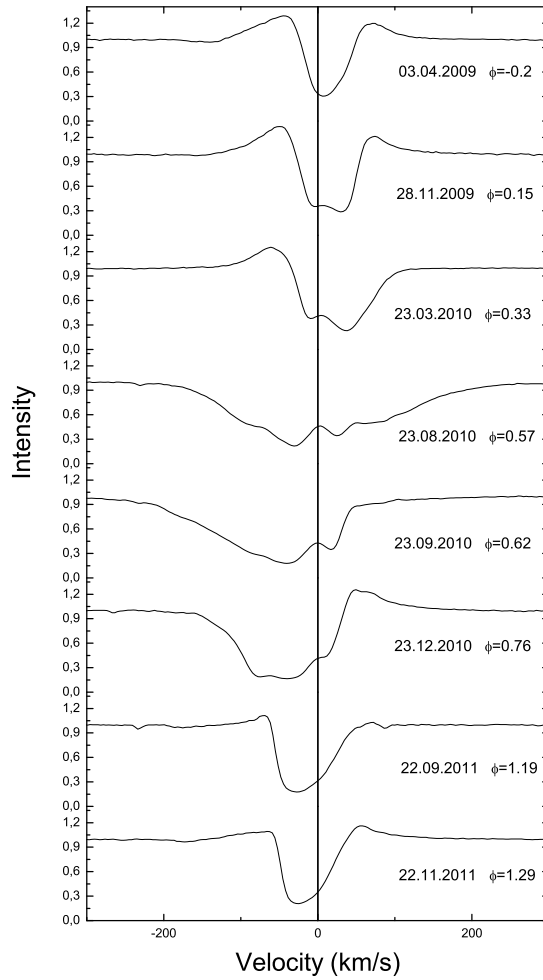


Figure 9: The H_{α} line profile variability during the eclipse.

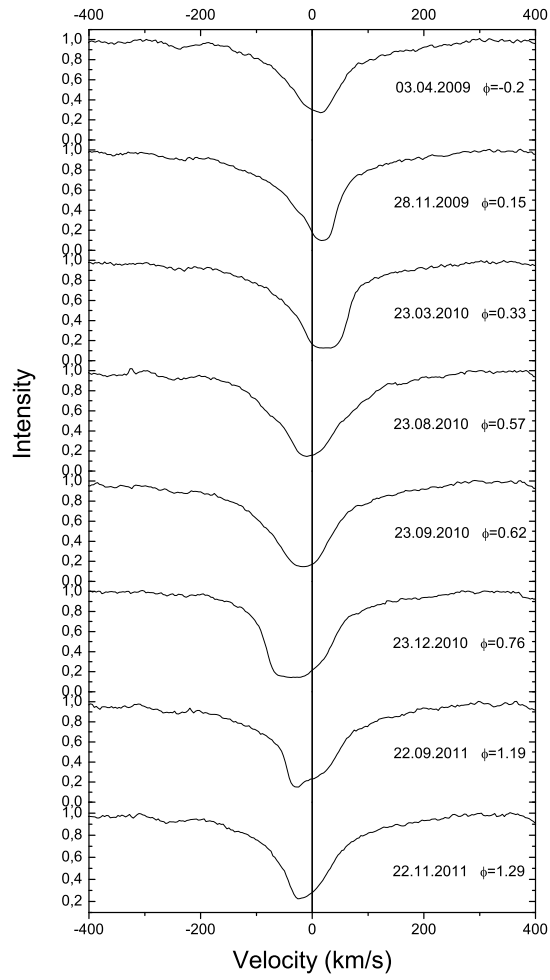


Figure 10: The H_δ line profile variability during the eclipse.

Literature

1. B. Kloppenborg, Ph.D. thesis, University of Denver (2012).
2. R.P. Stefanik, G. Torres, J. Lovegrove, V.E. Pera, D.W. Latham, J. Zajac, T. Mazeh, *Astrophys. J.*, **139**, 1254 (2010)
3. E.F. Guinan, L.E. DeWarf, in ASP Conf. Series, Vol. 279, Exotic Stars as Challenges to Evolution, ed. C. A. Tout & W. van Hamme (San Francisco: ASP), 121 (2002)
4. S.-S. Huang, *Astrophys. J.*, **141**, 976 (1965)
5. B. Kloppenborg, R.E. Stencel, J. Monnier et al., *Nature*, **464**, 870 (2010)
6. G. P. Kuiper, O. Struve, B. Stromgren, *Astrophys. J.*, **86**, 570 (1937)
7. O. Struve, H. Pillans, V. Zebergs, *Astrophys. J.*, **128**, 287 (1958)
8. D.L. Lambert, S.R. Sawyer, *PASP*, **98**, 389 (1986)
9. S. Ferluga, D. Mangiacapra, *Astron. and Astrophys.*, **243**, 230 (1991)
10. M. Saito, S. Kawabata, K. Saijo, H. Sato, *Publ. Astron. Soc. Japan*, **39**, 135 (1987)
11. P. Chadima, P. Harmanec, P.D. Bennett et al., *Astron. and Astrophys.*, **530**, A146 (2011b)
12. P. Chadima, P. Harmanec, S. Yang et.al., *IBVS*, 5937, 1 (2010)
13. R.E. Stencel, *JAAVSO*, vol. 40 (2012)
14. D. Tody, "IRAF in the Nineties" in *Astronomical Data Analysis Software and Systems II*, A.S.P. Conference Ser., Vol 52, eds. R.J. Hanisch, R.J.V. Brissenden, J. Barnes, 173 (1993)
15. G.A. Galazutdinov, *SAO Preprint*, 92 (1992)
16. Welty, D.E., Hobbs, L.M., *ApJS*, **133**, 345 (2001)
17. N. Mastrodemos, M. Morris, *Astrophys. J.* **497**, 303 (1998)
18. C. Guangwei, T. Huisong, X. Jun, L. Yongsheng, *Astron. and Astrophys.*, **284**, 874 (1994)
19. F. van Leeuwen, *Astron. and Astrophys.*, **474**, 653 (2007b)
20. E.F. Guinan, P. Mayer, P. Harmanec, et al., *Astron. and Astrophys.*, **546**, A123 (2012)
21. Th. Schmidt-Kaler, *The Physical Parameters of the Star*, in: Landolt-Bornstein, ed. K.-H. Hellwege, New Series Vol. VI, 2b, Springer, Berlin, Heidelberg, New York, p.1ff (1982)
22. P. van de Kamp, *Astron. J.*, **83**, 975 (1978)
23. D. W. Hoard, S. B. Howell, R. E. Stencel, *Astrophys. J.*, **714**, 549 (2010)
24. H. Kim, *JASS*, **25**, 1 (2008)
25. K. Sadakane, E. Kambe, B. Sato, S. Honda, O. Hashimoto, *Publ. Astron. Soc. Japan*, **62**, 1381 (2010)
26. Wilson, R.E., *Astrophys. J.* **170**, 529 (1971)
27. J.J.Lissauer, S.J.Wolk, C.A.Griffith, D.E.Backman, *Astrophys. J.*, **465**, 371 (1996)